Nucleic Acids Research, 2024, **52**, W306–W312
https://doi.org/10.1093/nar/gkae337
Advance access publication date: 30 April 2024
Web Server issue

RING 4.0: faster residue interaction networks with novel interaction types across over 35,000 different chemical structures

Alessio Del Conte [1], Giorgia F. Camagni [1], Damiano Clementel [1], Giovanni Minervini [1], Alexander Miguel Monzon [2], Carlo Ferrari [2], Damiano Piovesan [1,*] and Silvio C.E. Tosatto [1,*]

[1]Department of Biomedical Sciences, University of Padova, Padova, Italy
[2]Department of Information Engineering, University of Padova, Padova, Italy

[*]To whom correspondence should be addressed. Tel: +39 049 827 6269; Email: silvio.tosatto@unipd.it
Correspondence may also be addressed to Damiano Piovesan. Email: damiano.piovesan@unipd.it

Abstract

Residue interaction networks (RINs) are a valuable approach for representing contacts in protein structures. RINs have been widely used in various research areas, including the analysis of mutation effects, domain-domain communication, catalytic activity, and molecular dynamics simulations. The RING server is a powerful tool to calculate non-covalent molecular interactions based on geometrical parameters, providing high-quality and reliable results. Here, we introduce RING 4.0, which includes significant enhancements for identifying both covalent and non-covalent bonds in protein structures. It now encompasses seven different interaction types, with the addition of π-hydrogen, halogen bonds and metal ion coordination sites. The definitions of all available bond types have also been refined and RING can now process the complete PDB chemical component dictionary (over 35000 different molecules) which provides atom names and covalent connectivity information for all known ligands. Optimization of the software has improved execution time by an order of magnitude. The RING web server has been redesigned to provide a more engaging and interactive user experience, incorporating new visualization tools. Users can now visualize all types of interactions simultaneously in the structure viewer and network component. The web server, including extensive help and tutorials, is available from URL: https://ring.biocomputingup.it/.

Graphical abstract

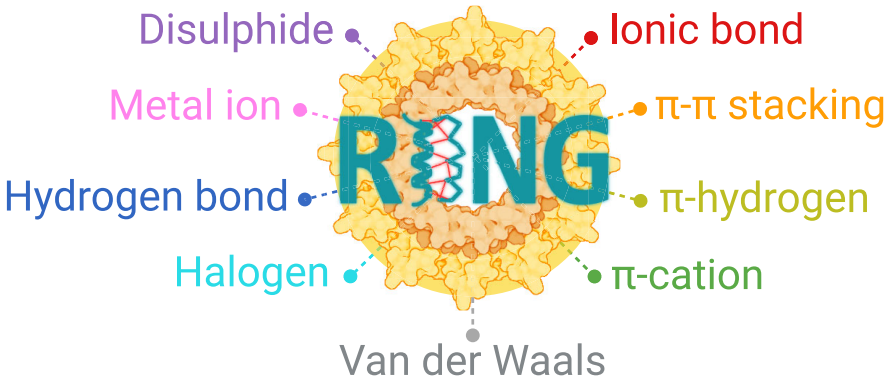

Introduction

Proteins are large macromolecules whose tridimensional structure and motion in conjunction with the molecular environment, provide the functional toolkit of the cell. Non-covalent interactions contribute to the stability of the folded structures (1), they are responsible for the interaction with other molecules in the formation of supra-molecular structures and are crucial in molecular communication such as allosterism and signaling processes, with the latter often mediated by transient interaction events (2).

Network theory provides an alternative approach to describe protein structures emphasizing the non-covalent protein's interactions. Residue interaction networks (RINs), also known as protein structure networks (PSNs), represent amino acids as nodes and the connections between them as edges (3). The definition of these connections, or contacts, typically takes into account parameters such as physico-chemical properties and geometrical constraints (distances and angles), enabling the analysis of the network properties and characterization of specific types of interactions.

Received: March 8, 2024. **Revised:** April 9, 2024. **Editorial Decision:** April 16, 2024. **Accepted:** April 19, 2024

Analysis of RINs is offered by a number of different solutions (4), of particular success is the Residue Interaction Network Generator (RING) which we have been developing and maintaining since 2011 (5–7).

The analysis of RINs has progressed from initially demonstrating the feasibility of network parameters in static structures to encompassing a range of more specialized applications.

In the last two years, RING has made significant contributions to numerous studies covering a diverse range of topics in protein research, including binding and allosterism, interfaces, protein stability, protein engineering, ligand binding prediction, software development and molecular dynamics analysis (8–10).

A recent study examines the relationship between the size of protein complex interfaces and the likelihood of cotranslational assembly. RING was employed to calculate contact-related properties of the interfaces, characterizing the different kinds of interactions between subunits (11).

Structural ensemble analysis is one of the main applications of RING. It is commonly used to analyze molecular dynamics simulations by calculating probabilistic contact networks (12,13), and to analyze protein stability and perform virtual screening (14,15).

Here, we present the new RING 4.0 version of the web server that has been redesigned to offer a more engaging and interactive user experience, including new visualization tools and additional data. The underlying software library has been optimized to enhance the calculation speed significantly. The software has been improved and is now able to process all the chemical compounds (>35 000 different molecules) available in the PDB chemical component dictionary. RING is now able to detect π-hydrogen and halogen bonds, as well as metal ion coordination types in addition to previously available types, whose definitions have been refined. RING 4.0 can now provide comprehensive interaction networks for various combinations of proteins, nucleotides, lipids, ligands, and small molecules and all different types of interactions can be visualized in the structure viewer and in a graph representation simultaneously.

Materials and methods

The RING web server has at its core the RING application, which has been extensively modified and improved compared to the previous version (7). In terms of calculating interactions, advancements were made to align with current standards. This involved broadening calculations to include any ligand present in the PDB database, and introducing novel interaction categories. Additionally, we improved the execution time of about one order of magnitude. In the following, we explain what changes have been introduced since the previous version, to the application and the web server.

Structure internal representation

The RING application takes as input protein structures, in the format of PDB or PDBx/mmCIF file, requiring parsing and conversion into an internal protein representation.

This internal representation aims to accurately reflect the composition and chemical connectivity between atoms necessary for interaction calculations. In the new version of RING we expanded connectivity calculations beyond amino acids and nucleic acids in order to detect typed interactions for all possible compounds. Compounds chemical bonds and aromaticity are taken as external input from the PDB Chemical Component Dictionary (CCD) (16) that contains over 35 000 entries and covers all structures available in the PDB. After establishing atom connections, a Depth First Search (DFS) algorithm is employed to identify all possible rings, which are then filtered based on the presence of all atoms listed as aromatic in the CCD and their coplanarity within a fixed threshold.

RING can place hydrogen atoms in those input structures lacking them, as the presence of hydrogens is crucial for many interactions. When missing, RING can add hydrogens coordinates based on the bond angle and dihedral angle with the neighboring atoms. Since angles are fixed parameters and depend on the type of atoms involved, in the new RING version we retrieved all possible parameters for all compounds available in the PDB and stored them in a helper file.

During atom loading, various properties are assigned to them. These properties include their van der Waals radius, which has been expanded to encompass all known radii, as well as indicators specifying whether an atom is a metal ion or a halogen atom.

The integration of these data files into RING alleviates the burden of real-time parameter calculations, mitigating the execution time and possible errors. Moreover, users retain the flexibility to modify this information as needed for customized chemical components. When new compounds (not available in the PDB) are analyzed, connectivity information, including hydrogen placement, can be directly provided by the user.

Non-covalent bond calculation

In the latest version, significant modifications have been made to the majority of prior interactions, including hydrogen bonding (17), π–π stacking (18), π–cation interactions (19) and van der Waals interactions. These changes were motivated by several factors: expanding the definition of the interactions to encompass all chemical components where feasible, optimizing the software's performance, and finally to align with the latest advancements in defining non-covalent bonds as per state-of-the-art publications.

Additionally, three new categories of interactions have been introduced: the π–hydrogen bond (20), halogen bonds where the acceptor can be an atom containing a lone pair of electrons (21) or a π system (22), and the metal ion coordination (23). For a comprehensive understanding of how these interactions are computed, please consult the documentation available on the web server (https://ring.biocomputingup.it/about).

Execution time

In this updated version, significant improvements have been made to the overall performance of the application. Previously, the implementation was designed to be versatile across different uses, which meant the data structure was not well-optimized for specific tasks. The latest update brings significant enhancements to the software's underlying logic and data structures, resulting in a significant decrease in both memory accesses and execution time. These improvements are facilitated by the implementation of efficient data structures like hash maps, known for their average constant-time complexity in operations such as search, insertion, and removal of elements. This optimization expands the software's utility beyond standard amino acids and nucleic acids, while also incor-

porating the latest C++ standards to enrich the overall APIs. Addressing performance issues, we utilized advanced profilers like perf (https://perf.wiki.kernel.org), which allowed us to identify and address time-consuming segments through iterative refinement of algorithms and optimization of memory utilization, including the management of heap memory.

For instance, processing times for complex structures like the RNA polymerase-Gfh1 (PDB code: 3aoh) have been notably reduced, with RING 4 completing computations in just 3.2 s compared to the 22 s required by RING 3.0. Similarly, handling larger structures such as the Virus-like particle of bacteriophage AC (PDB code 6yf7) is now accomplished in a mere 5.9 s, a considerable improvement over the 33 s previously needed. Even for conformational ensembles like the dihydrofolate reductase with multiple models (PDB code: 4p3r), RING 4 demonstrates its efficiency, completing computations in 9 s as opposed to the 30 s taken by RING 3.0.

Web-server implementation

The web server utilizes DRMAAtic (https://drmaatic.biocomputingup.it) as its backend, an in-house solution designed for executing jobs remotely using our cluster infrastructure. DRMAAtic interfaces with the SLURM (24) scheduler via the Distributed Resource Manager Application API (25), managing job submission, permissions, user management, and file retrieval. It incorporates throttling mechanisms to prevent service misuse. Built on the Django REST Framework (26) that provides most of the functionality to create the REST APIs that are then used by the front-end interface to submit the jobs and download the results. DRMAAtic facilitates the creation of REST APIs utilized by the front-end interface for job submission and result retrieval. Authentication to DRMAAtic is achieved through OAuth 2.0 implicit flow, with ORCID (https://orcid.org/) serving as the identity provider.

The RING web-server

Leveraging on DRMAAtic's capabilities, the web server's front-end interface enables users to submit RING jobs with customizable parameters and inputs, it will track the status of the job, and retrieve the results when available. Users can login to save submitted jobs to their account for easy retrieval across different devices. The web server functions fully without requiring user registration; past jobs are stored in the browser's cookies and can be associated with the account upon login.

Input

The home page of the web-server offers to the user an introduction to what RING is, and an input form that can be used for submitting new jobs. The form accepts as input a structure file as PDB or PDBx/mmCIF formats, or an identifier that can be both from the PDB (27) or AlphaFold DB (28). In the latter case, an autocomplete of the two has been implemented. After selecting an input structure, the user can modify different parameters, such as the chain to analyze (by default all chains are considered), the model number (in case of multiple state structure, all models are considered by default), and many other options to change the interactions thresholds or apply filters. While RING in principle has no limitations in the number of models that can be processed, due to restrictions in visualizing large structures, only files of up to 200 MB in size are accepted by the server. For larger structural ensembles we recommend installing RING locally. Finally, if the job submission passes all server checks, the user is redirected to the result page, which checks the job status and reloads until it completes. Otherwise an error message is displayed.

Output

When the RING job is finished, the front-end presents the outputs across various graphic components, to highlight different aspects of the results. These include a 3D structure viewer built with the Mol* Viewer (29), an interactive graph, representing residues as nodes, and the interactions as edges and a conformational dependent contact map, available only when the input has multiple states, shows for each residue if the selected interaction is present or not in a state.

The new version of the output page has been improved in several ways. First, the structure viewer has been enhanced to reveal RING contacts and their associated details when focusing on specific residues on the graph. Second, we created a probability contact map represented as a matrix highlighting interacting residue pairs and their likelihood of contact across multiple states.

Third, we integrated a contact table that lists interacting residue pairs categorized by contact type, with probabilities for multi-state inputs.

Notably, the structure viewer and the graph module can be customized, it is possible to filter the interactions that are displayed based on parameters like type, intra-chain or inter-chain designation, and interaction frequency for multi-state structures.

Users can also adjust residue color schemes based on properties such as chain, type, sequence position, secondary structure (DSSP) assignment, and node degree. Notably, all components are tightly connected to each other enabling seamless navigation; selecting a residue or interaction in one component automatically highlights it across others, facilitating focused analysis for users.

The user can easily access and download various results, including the original outputs generated by RING, its conversion into a network saved in JSON file format, SVG or high-resolution screenshots for other components, as well as tabular exports for the contact maps and tables.

Contact type distribution in PDB structures

We downloaded from the PDB (updated to February 2024) all the structures with a resolution ≤1.6 Å, corresponding to 31 229 PDB structures. We executed RING on all these structures, and analyzed the distribution of contacts for different classes of interactions. In Table 1, we reported the distribution of contacts detected by RING, excluding results of PDB entries without protein chains, therefore limiting the analysis to 31 144 PDB structures, comprising 10 032 different proteins (different UniProt identifiers). For proteins, we exclusively consider standard amino acids, while for ligands, all non-amino acid entities are included, and for nucleic acids, both DNA and RNA bases are encompassed. Instead of using the 'auth_asym_id' attribute, which corresponds to the chain identifier in the canonical PDB format, we opted to consider the value provided by the 'label_asym_id' attribute in the mmCIF format as chain identifiers. This decision was made as the same chain identifier in the PDB format can be used to store different molecular entities that are not necessarily covalently

Table 1. Distribution of RING contacts in high-resolution PDB structures

	Intra-chain				Inter-chain					
Interaction partners	**AA-AA**		**AA-Ligand^**		**AA-AA**		**AA-Ligand**		**AA-Nucleic acid**	
Number of PDBs	30 244		3166		12 605		25 062		462	
Number of contacts	9 431 609		33 074		300 687		324 296		9311	
Hydrogen bond	8 442 301	89.5%	31 410	95.0%	229 295	76.3%	229 855	70.9%	8517	91.5%
π-π stacking	620 405	6.6%	1475	4.5%	36 301	12.1%	33 175	10.2%	608	6.5%
π-cation	87 262	0.9%	102	0.3%	7278	2.4%	2836	0.9%	180	1.9%
Ionic bond	234 741	2.5%	–	–	25 025	8.3%	–	–	–	–
Disulfide	23 526	0.2%	–	–	890	0.3%	–	–	–	–
π-hydrogen bond*	23 374	0.2%	35	0.1%	1898	0.6%	962	0.3%	6	0.1%
Halogen bond*	–	–	43	0.1%	–	–	831	0.3%	–	–
Metal ion coordination*	–	–	–	–	–	–	56 637	17.5%	–	–

Only contacts involving at least one amino acid (AA) as an interacting partner are reported. Each column represents distinct interaction partners, and it is indicated whether the interacting groups are in the same chain (Intra-chain) or different chains (Inter-chain). The 'Number of PDBs' refers to the total number of PDB structures in which the interaction has been observed. For categorized interactions, we also provide the fraction of contacts observed for each category. The statistics are derived by considering the 'label_asym_id' attribute in the mmCIF format as chain identifiers. (*) Interaction types introduced in the new version of the RING software. (^) The intra-chain AA-Ligand column includes cases where standard amino acids interact with non-standard amino acids of the same chain. Currently, non-standard amino acids are automatically processed by RING as ligands. However, in the current implementation of RING, ionic bonds are detected only when amino acids are involved, and π-cation interactions are detected only when the cation is on the amino acid partner. Therefore, their contribution in ligand interactions is missing.

bonded. By using the 'label_asym_id' attribute, we avoid the potential pitfalls of inaccurate statistics and incorrect attribution of many inter-chain interactions to the intra-chain class. Both the web server and the RING executable now offer the option to choose which field to consider for the selection of the chain identifier.

The analysis of non-covalent contacts across biomolecular interactions in Table 1 unveils notable trends.

Hydrogen bonds emerge as ubiquitous as expected. The difference in the percentage of intra- and inter-chain AA–AA hydrogen bonds (89.5% and 76.3%) could be explained by the different roles of this type of interaction in different contexts. Intra-chain hydrogen bonds are predominant in the stabilization of secondary structure elements, whereas surface inter-chain interactions in protein-protein complexes are stabilized by a more heterogeneous set of contacts that include a significant fraction of π–π stacking (12.1%) and π–cation (2.4%) contacts among others.

π–π stacking prominently characterizes both protein–protein (AA-AA) and protein–ligand (AA–ligand) inter-chain interactions, indicating their importance in the stabilization of supramolecular complexes.

Although the π–hydrogen bond is relatively uncommon (0.3%, inter-chain AA–ligand), its presence in interactions between proteins and ligands emphasizes its potential significance in stabilizing particular structural patterns. Protein–ligand π–π stacking and π–hydrogen bonds are now detected by the new version of RING for the first time thanks to the fact that the software is now able to recognize aromatic rings for all known PDB ligands.

As an example, RING was able to detect a very rare π–hydrogen contact between an amino acid of the 50S ribosomal protein L33 (PHE 39, label_asym_id/chain A) and a base of a 23S rRNA (G 2374, label_asym_id/chain BA) of the 8b0a PDB.

Metal ion coordination stands out prominently in ligand interactions (AA–ligand) accounting for 17.5% of the total inter-chain interactions. This highlights the significant role of ionic coordination in molecular recognition and binding.

Finally, halogen bonds are extremely rare (0.3%) and only observed in protein–ligand interactions.

Despite the great improvement in the classification of contacts involving a ligand molecule, RING in its current implementation still presents some limitations. The software provides ionic bonds exclusively for amino acids, therefore ionic contacts are not detected in protein–ligand complexes. Moreover, RING detects π–cation interactions only when the cation is on the amino acid partner, therefore their abundance is underestimated when a ligand is involved.

In conclusion, the three new types of interactions introduced (metal ion coordination, π–hydrogen bond and halogen bond) expand RING capacity of investigating processes such as molecular recognition and protein–ligand binding.

Use case

The use case studies reported below illustrate how the new RING version can extract valuable biological information from molecular interactions.

The androgen receptor (AR) is a ligand-dependent transcription factor involved in male sexual development and the etiology of pancreatic cancer (PCa). Therefore, it is considered an excellent pharmacological target for the treatment of prostate cancer. An X-ray crystallography study (PDB code: 8e1a) of AR in complex with the antagonist compound VPC14368 is presented in Figure 1A. The receptor comprises three main functional domains: an N-terminal domain (NTD), a highly conserved DNA binding domain (DBD), and a C-terminal ligand binding domain (LBD). VPC14368 binds to the androgen binding site (ABS) located in the LBD.

RING generates a comprehensive network of interactions between the protein and ligand, also expanding on intra-chain protein-ligand interactions which were excluded in the previous version. This facilitates the study of molecular details governing the AR-LBD ligand interaction (Figure 1A). The compound highlighted in the figure is stabilized in the binding pocket by a network of electrostatic interactions, including van der Waals and aromatic interactions. The phenyl ring of the ligand forms van der Waals interactions (gray) with the surrounding side chains of M749, V746 and F764, establishing a π–π stack interaction (orange). The thiazole ring is

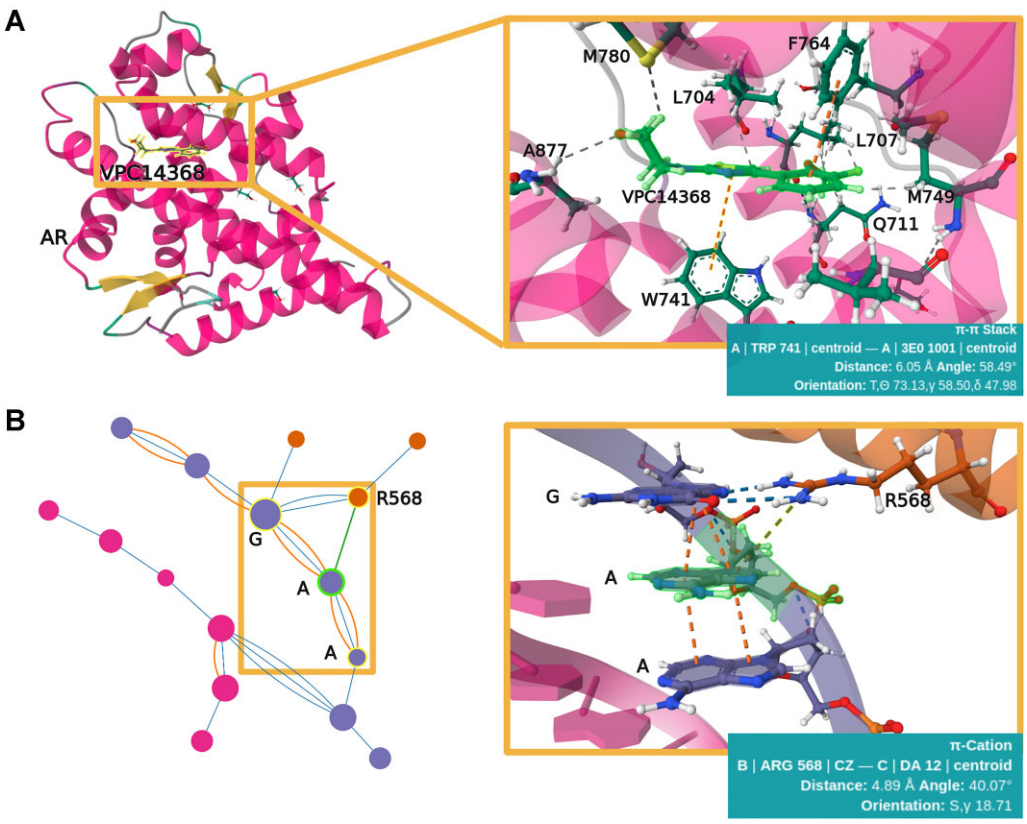

Figure 1. Molecular insights into androgen receptor (AR) interactions calculated by RING 4.0. (**A**) AR-LBD complex with antagonist compound VPC14368 (PDB code: 8e1a) highlights electrostatic, van der Waals, and aromatic interactions. (**B**) AR's DNA-binding domain (DBD) bound to DNA (PDB code: 1r4i) showcases hydrogen bonding and π-cation interactions crucial for DNA recognition.

stabilized by an electrostatic interaction with L704 and a π–π stack with W741. Additionally, the morpholine group interacts with the side chains of M780 and A877 via van der Waals interactions (Figure 1A).

As a transcription factor, the androgen receptor, when activated by endogenous ligands (testosterone and 5α-dihydrotestosterone (DHT)), translocates into the nucleus and initiates the transcription of target genes. In Figure 1B, the crystallized structure of the AR DNA-Binding Domain bound to the Direct Repeat Response Element (PDB code: 1r4i) is depicted. An interaction involving the R568 residue includes two hydrogen bonds (blue) with guanine and a π-cation interaction (green) with the underlying selected nitrogenous base, adenine. Furthermore, the α-helix, colored in purple, is stabilized by π–π stack interactions between the nitrogenous bases.

RING 4.0 not only provides information on protein-protein interactions but also offers molecular details on protein-ligand and protein-nucleic acid interactions. This information can be utilized to study differences in endogenous protein-ligand and protein-inhibitor interactions or guide the structure-based design of new molecules targeting specific proteins.

Conclusions

RING has become a milestone for generating the increasingly popular residue interaction networks. The RING web interface has been re-designed to provide a richer and more interactive user experience, with novel visualization aids as well as more data. The help and about pages have been significantly expanded to cover the new features.

This new version extends the previous server RING in several ways. First of all, the underlying software library has been carefully optimized to make the software about one order of magnitude faster than RING 3.0 (or about 100 times faster than RING 2.0).

Usage of the complete PDB chemical component dictionary now provides the full range of 10 different non-covalent bond types for over 35 000 different chemical compounds including all known ligands. Of relevance, we have added π–hydrogen and halogen bonds as well as metal ion coordination types. Together with tightened definitions for all other non-covalent bond types, RING 4.0 is now able to provide rich interaction networks for any combination of protein, nucleotides, lipids, ligands and small molecules. RING aims to deepen our understanding of the intricate interplay of molecular forces in governing biomolecular stability and function, offering valuable insights for drug design and molecular engineering endeavors.

The RING server is included in the Service Delivery Plan of ELIXIR-Italy, implying a strong commitment to its continued availability over the coming years.

Data availability

No new data were generated or analysed in support of this research. The web server, including extensive help and tutorials, is available from URL: https://ring.biocomputingup.it/.

Funding

ELIXIR, the research infrastructure for life science data; COST Action ML4NGP [CA21160], supported by COST (European Cooperation in Science and Technology); European Union's Horizon 2020 research and innovation programme [823886 MSCA-RISE 'REFRACT']; European Union through NextGenerationEU, PNRR project ELIXIRxNextGenIT [IR0000010]; National Center for Gene Therapy and Drugs based on RNA Technology [CN00000041]; Fondazione AIRC per la Ricerca sul Cancro (AIRC) [MFAG 29017 and IG 2019 ID 23825]; Italian Ministry of Education and Research through the NextGenerationEU fund PRIN 2022 project: PLANS [2022W93FTW]. Funding for open access charge: University of Padova.

Conflict of interest statement

None declared.

References

1. Dill,K.A. and MacCallum,J.L. (2012) The protein-folding problem, 50 years on. *Science*, **338**, 1042–1046.
2. del Sol,A., Fujihashi,H., Amoros,D. and Nussinov,R. (2006) Residues crucial for maintaining short paths in network communication mediate signaling in proteins. *Mol. Syst. Biol.*, **2**, 2006.0019.
3. del Sol,A. and Carbonell,P. (2007) The modular organization of domain structures: insights into protein-protein binding. *PLoS Comput. Biol.*, **3**, e239.
4. Liang,Z., Verkhivker,G.M. and Hu,G. (2020) Integration of network models and evolutionary analysis into high-throughput modeling of protein dynamics and allosteric regulation: theory, tools and applications. *Briefings Bioinf.*, **21**, 815–835.
5. Martin,A.J.M., Vidotto,M., Boscariol,F., Domenico,T.D., Walsh,I. and Tosatto,S.C.E. (2011) RING: Networking interacting residues, evolutionary information and energetics in protein structures. *Bioinformatics*, **27**, 2003–2005.
6. Piovesan,D., Minervini,G. and Tosatto,S.C.E. (2016) The RING 2.0 web server for high quality residue interaction networks. *Nucleic Acids Res.*, **44**, W367–W374.
7. Clementel,D., Del Conte,A., Monzon,A.M., Camagni,G.F., Minervini,G., Piovesan,D. and Tosatto,S.C.E. (2022) RING 3.0: fast generation of probabilistic residue interaction networks from structural ensembles. *Nucleic Acids Res.*, **50**, W651–W656.
8. Verkhivker,G., Agajanian,S., Kassab,R. and Krishnan,K. (2022) Probing mechanisms of binding and allostery in the SARS-CoV-2 spike omicron variant complexes with the host receptor: revealing functional roles of the binding hotspots in mediating epistatic effects and communication with allosteric pockets. *Int. J. Mol. Sci.*, **23**, 11542.
9. Guo,H.-B., Varaljay,V.A., Kedziora,G., Taylor,K., Farajollahi,S., Lombardo,N., Harper,E., Hung,C., Gross,M., Perminov,A., *et al.* (2023) Accurate prediction by AlphaFold2 for ligand binding in a reductive dehalogenase and implications for PFAS (per- and polyfluoroalkyl substance) biodegradation. *Sci. Rep.*, **13**, 4082.
10. Krishnan,K., Tian,H., Tao,P. and Verkhivker,G.M. (2022) Probing conformational landscapes and mechanisms of allosteric communication in the functional states of the ABL kinase domain using multiscale simulations and network-based mutational profiling of allosteric residue potentials. *J. Chem. Phys.*, **157**, 245101.
11. Badonyi,M. and Marsh,J.A. (2022) Large protein complex interfaces have evolved to promote cotranslational assembly. *eLife*, **11**, e79602.
12. Sakai,T., Mashima,T., Kobayashi,N., Ogata,H., Duan,L., Fujiki,R., Hengphasatporn,K., Uda,T., Shigeta,Y., Hifumi,E., *et al.* (2023) Structural and thermodynamic insights into antibody light chain tetramer formation through 3D domain swapping. *Nat. Commun.*, **14**, 7807.
13. Petrizzelli,F., Biagini,T., Bianco,S.D., Liorni,N., Napoli,A., Castellana,S. and Mazza,T. (2022) Connecting the dots: a practical evaluation of web-tools for describing protein dynamics as networks. *Front Bioinform*, **2**, 1045368.
14. Ramakrishnan,K., Johnson,R.L., Winter,S.D., Worthy,H.L., Thomas,C., Humer,D.C., Spadiut,O., Hindson,S.H., Wells,S., Barratt,A.H., *et al.* (2023) Glycosylation increases active site rigidity leading to improved enzyme stability and turnover. *FEBS J.*, **290**, 3812–3827.
15. Kongsompong,S., E-Kobon,T., Taengphan,W., Sangkhawasi,M., Khongkow,M. and Chumnanpuen,P. (2023) Computer-aided virtual screening and in vitro validation of biomimetic tyrosinase inhibitory peptides from abalone peptidome. *Int. J. Mol. Sci.*, **24**, 3154.
16. Westbrook,J.D., Shao,C., Feng,Z., Zhuravleva,M., Velankar,S. and Young,J. (2015) The chemical component dictionary: complete descriptions of constituent molecules in experimentally determined 3D macromolecules in the Protein Data Bank. *Bioinformatics*, **31**, 1274–1278.
17. Torshin,I.Y., Weber,I.T. and Harrison,R.W. (2002) Geometric criteria of hydrogen bonds in proteins and identification of `bifurcated' hydrogen bonds. *Protein Eng. Des. Select.*, **15**, 359–363.
18. Zhao,Y., Li,J., Gu,H., Wei,D., Xu,Y., Fu,W. and Yu,Z. (2015) Conformational preferences of π–π stacking between ligand and protein, analysis derived from crystal structure data geometric preference of π–π interaction. *Interdiscip. Sci. Comput. Life Sci.*, **7**, 211–220.
19. Infield,D.T., Rasouli,A., Galles,G.D., Chipot,C., Tajkhorshid,E. and Ahern,C.A. (2021) Cation-π Interactions and their Functional Roles in Membrane Proteins. *J. Mol. Biol.*, **433**, 167035.
20. Steiner,T. and Koellner,G. (2001) Hydrogen bonds with π-acceptors in proteins: frequencies and role in stabilizing local 3D structures. *J. Mol. Biol.*, **305**, 535–557.
21. Chen,Z., Wang,G., Xu,Z., Wang,J., Yu,Y., Cai,T., Shao,Q., Shi,J. and Zhu,W. (2016) How do distance and solvent affect halogen bonding involving negatively charged donors? *J. Phys. Chem. B*, **120**, 8784–8793.
22. Shah,M.B., Liu,J., Zhang,Q., Stout,C.D. and Halpert,J.R. (2017) Halogen−π interactions in the cytochrome P450 active site: structural insights into human CYP2B6 substrate selectivity. *ACS Chem. Biol.*, **12**, 1204–1210.
23. Zheng,H., Cooper,D.R., Porebski,P.J., Shabalin,I.G., Handing,K.B. and Minor,W. (2017) CheckMyMetal: a macromolecular metal-binding validation tool. *Acta Crystallogr. D Struct. Biol.*, **73**, 223–233.
24. Yoo,A.B., Jette,M.A. and Grondona,M. (2003) SLURM: Simple Linux Utility for Resource Management. In: Feitelson,D., Rudolph,L. and Schwiegelshohn,U. (eds.) *Job Scheduling Strategies for Parallel Processing, Lecture Notes in Computer Science*. Springer Berlin Heidelberg, Berlin, Heidelberg, Vol. **2862**, pp. 44–60.
25. Troger,P., Rajic,H., Haas,A. and Domagalski,P. (2007) Standardization of an API for distributed resource management systems. In: *Seventh IEEE International Symposium on Cluster Computing and the Grid (CCGrid '07)*. pp. 619–626.
26. Tom Christie and Open source community (2022) *Django REST Framework*. Version 3.14.
27. Burley,S.K., Bhikadiya,C., Bi,C., Bittrich,S., Chen,L., Crichlow,G.V., Christie,C.H., Dalenberg,K., Di Costanzo,L., Duarte,J.M., *et al.* (2021) RCSB Protein Data Bank: powerful new tools for exploring 3D structures of biological macromolecules for basic and applied research and education in fundamental biology,

biomedicine, biotechnology, bioengineering and energy sciences. *Nucleic Acids Res.*, **49**, D437–D451.
28. Varadi,M., Anyango,S., Deshpande,M., Nair,S., Natassia,C., Yordanova,G., Yuan,D., Stroe,O., Wood,G., Laydon,A., *et al.* (2022) AlphaFold Protein Structure Database: massively expanding the structural coverage of protein-sequence space with high-accuracy models. *Nucleic Acids Res.*, **50**, D439–D444.
29. Sehnal,D., Bittrich,S., Deshpande,M., Svobodová,R., Berka,K., Bazgier,V., Velankar,S., Burley,S.K., Koča,J. and Rose,A.S. (2021) Mol* Viewer: modern web app for 3D visualization and analysis of large biomolecular structures. *Nucleic Acids Res.*, **49**, W431–W437.

Received: March 8, 2024. **Revised:** April 9, 2024. **Editorial Decision:** April 16, 2024. **Accepted:** April 19, 2024